FT-IR and Raman microscopic study at 293 K and 77 K of celestine, SrSO$_4$, from the middle triassic limestone (Muschelkalk) in Winterswijk, The Netherlands

J. Theo Kloprogge[1*], Huada Ruan[1], Loc V. Duong[1,2] and Ray L. Frost[1]

[1] Centre for Instrumental and Developmental Chemistry, Faculty of Science, Queensland University of Technology, 2 George Street, GPO Box 2434, Brisbane Q 4001, Australia
[2] Analytical Electron Microscopy Facility, Faculty of Science, Queensland University of Technology, 2 George Street, GPO Box 2434, Brisbane Q 4001, Australia

* Corresponding author: phone +61 7 3864 2184, fax +61 7 3864 1804, E-mail t.kloprogge@qut.edu.au

Abstract

This paper describes the Raman and infrared spectroscopy of SrSO$_4$ or celestine from the Muschelkalk of Winterswijk, The Netherlands. The infrared absorption spectrum is characterised by the SO$_4^{2-}$ modes ν_1 at 991 cm^{-1}, ν_3 at 1201, 1138 and 1091 cm^{-1}, and ν_4 at 643 and 611 cm^{-1}. An unidentified band is observed at 1248 cm^{-1}. In the Raman spectrum at 293 K the ν_1 mode is found at 1000 cm^{-1} and is split in two bands at 1001 and 1003 cm^{-1} upon cooling to 77 K. The ν_2 mode, not observed in the infrared spectrum, is observed as a doublet at 460 and 453 cm^{-1}. The ν_3 mode is represented by four bands in the Raman spectrum at 1187, 1158, 1110 and 1093 cm^{-1} and the ν_4 mode as three bands at 656, 638 and 620 cm^{-1}. Cooling to 77 K results in a general decrease in bandwidth and a minor shift in frequencies. A decrease in intensities is observed upon cooling to 77 K due to movement of the Sr atom towards one or more of the oxygen atoms in the sulfate group.

Key words: celestine, infrared spectroscopy, Raman microscopy, strontium sulfate

Introduction

Celestine (sometimes also referred to as celestite), Sr-SO$_4$, is the most important source of strontium and is mostly found in fissures and cavities in dolomites and dolomitic limestones, although formation in evaporite deposits is also known. Celestine got its name from its bluish colour as the Latin word *caelestis* means sky (blue). The structure of celestine is identical to that of barite, BaSO$_4$, with Sr^{2+} taking the place of Ba^{2+}. The SO$_4^{2-}$ ions are approximately regular tetrahedra lying with the S and O atoms on mirror planes at y = 0 and y = 1/2. The other two O atoms are equidistant from and on opposite sites of these mirror planes. The Sr atoms also lie on the mirror planes and link the sulfate ions in such a way that each Sr atom is coordinated by 12 O atoms.

Celestine was found and reported for the first time in the Middle Triassic limestones (Muschelkalk) of Winterswijk in 1974 by two amateur geologists (Habers and Tangerding 1975, Habers 1982). The first finds contained clear blue crystals in fissures formed due to lateral secretion on both sides of the fissures. Later also geode-like cavities were found with more reddish idiomorphic celestine crystals, often accompanied by white calcite crystals. The reddish colour is probably caused by iron hydroxide from the top layer (Peletier and Kolstee 1986, Oosterink 1986).

Infrared spectra of anhydrous sulfates like celestine and hydrous sulfates like gypsum have been studied for a long time (see e.g. Omori 1968, Guirguis 1987, Rull et al. 1989, Kloprogge and Frost 1999a). Frequencies of the fundamental modes of the SO$_4$ ion differ from those observed for various minerals like barite, celestine, anglesite, gypsum and anhydrite (Ross 1972, Gadsden 1975, Griffith 1987) and other compounds like basic aluminium sulfate (Kloprogge

and Frost 1999b,c). In many of these compounds the site symmetry of the sulfate is sufficiently low to activate all nine infrared active vibrations (Ross 1972). Adler and Kerr (1965) have discussed the spectra of the anhydrous sulfates of Sr, Ba and Pb. They observed shifts to lower frequencies of the stretching vibrations with increasing cation mass. Most of these minerals also give strong and sharp Raman bands due to strong polarisability of the metal-oxygen bond in addition to the fundamental sulfate bands. Raman spectra of celestine have only been very scarcely reported. Rull et al. (1989) have reported the Raman and infrared spectra of some Spanish celestines, but until now nobody has reported the spectra of Dutch celestine. Therefore, this paper contains the first Raman and infrared spectra of Dutch celestine. In addition Raman microscopy at liquid nitrogen temperature has been applied in order to gain a more thorough knowledge of the Raman spectrum as lowering of the temperature often results in sharpening of the bands and a shift of the bands towards either higher or lower frequency resulting in a possible increased band separation (enhanced "pseudo-resolution").

Theoretical analysis

Celestine crystallises in the orthorhombic system $Pnma$ with a 8.35 Å, b 5.35 Å and c 6.87 Å ($Z = 4$). This leads to a space group of with site group C_s for the sulfate group. SO_4 has theoretically 9 degrees of vibrational freedom (Table 1):

$$\tilde{A}_{vib} = 6A' + 3A'' \text{ (Ross 1972)}$$

All these vibrations are potentially Raman and infrared active. The Raman spectrum of SO_4^{2-} in solutions (site symmetry T_d) shows fundamental vibrations at 981 (v_1), 451 (v_2), 1104 (v_3) and 613 cm^{-1} (v_4). However, in the crystal structure of celestine the symmetry of the perfect tetrahedron is lowered, resulting in splitting of especially the v_3 and v_4 modes.

Experimental

Origin of the sample

The celestine used in this study is the reddish variety found in 1985 by one of the authors (JTK) in at that time the most western quarry in the Muschelkalk of Winterswijk. In addition to the celestine crystals, white crystals of calcite are present in the sample. A few celestine crystals were removed from a cavity for the FTIR measurements as for the Raman microscopic measurements. Cleaning of the crystal for the Raman microscopy was not necessary. Analysis with a JEOL 840A Electron Proble Microanalyser of these crystals revealed that the large celestine crystals (Fig. 1a) contain no substitution of Sr by other cations such as Ba.

However, the surface of these crystals have been subjected to dissolution processes resulting in the formation of etch pits in the shape of negative crystals. On the surface of these crystals a second generation of sulphate crystals have been formed that, in contrast are rich in both Ba and Sr. This indicates that the Ba has been introduced in the system at a later stage, where it crystallized together with the dissolved Sr and sulphate from the celestine. This Ba-rich second phase is observed as either very small crystals with an average diameter of 10 μm (Fig 1b) and as aggregates up to 100 μm (Fig 1c). The chemical analyses are summarized in Table 2. The iron hydroxide, which has been reported to cause the reddish colour, could not be observed in the sample.

Fourier transform infrared spectroscopy

The celestine sample was ultrasonically cleaned and finely ground for one minute, combined with oven dried spectroscopic grade KBr (containing approximately 1 wt% celestine) having a refractive index of 1.559 and a particle size of 5-20 μm (300 mg) and pressed into a disc under vacuum. The spectrum of each sample was recorded in triplicate by accumulating 512 scans at 4 cm^{-1} resolution between 400 cm^{-1} and 4000 cm^{-1} using the Perkin-Elmer 1600 series

Table 1. Correlation table for the possible vibrations of tetrahedral SO_4^{2-} (Ross 1972; 1974).

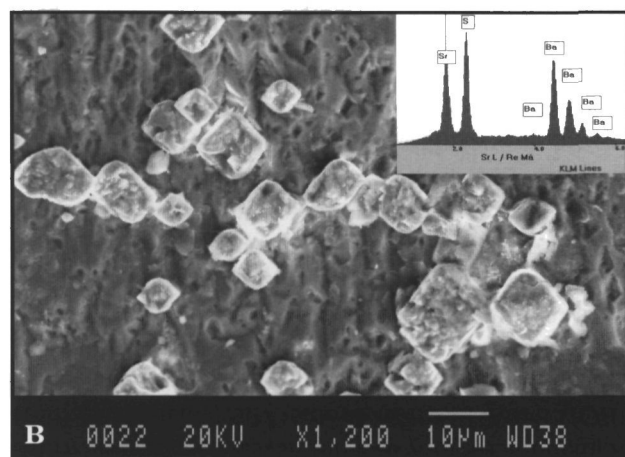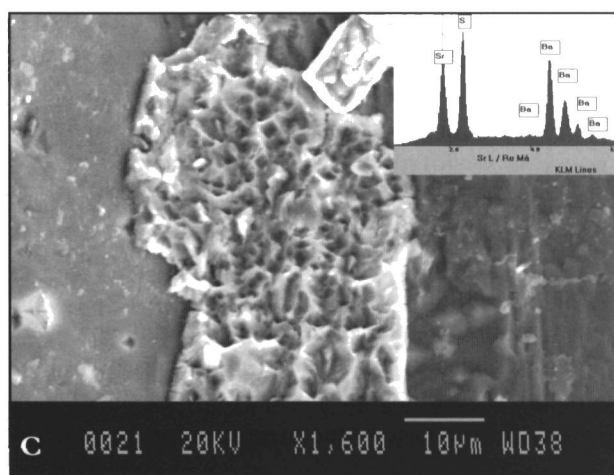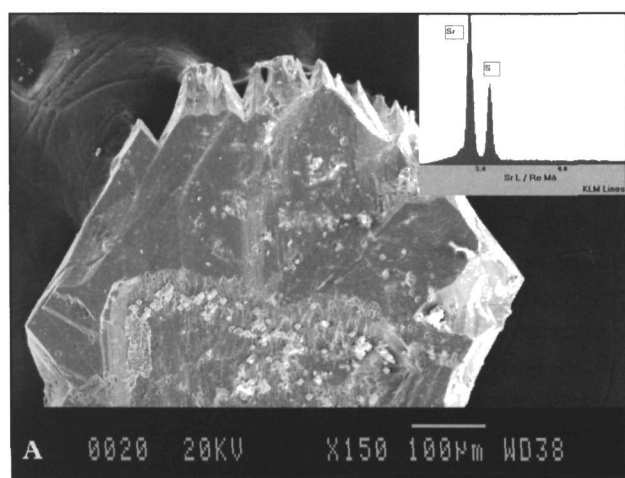|	Site symmetry	Mode and symmetry class			activity		
		v_1	v_2	v_3, v_4	Raman active only	Raman + IR active	No. of IR active bands
Free SO_4^{2-}	T_d	A_1	E	F_2	A_1, E	F_2	2
Celestine	C_s	A'	$A' + A''$	$2A' + A''$	–	A', A''	9

Fig. 1. Scanning electron microscope images of a) large celestine crystals, b) small second phase sulphate crystals and c) aggregate of second phase crystals.

Fourier transform infrared spectrometer equipped with a LITA detector.

Raman microscopy

Small amounts of celestine crystals were placed on a polished metal surface on the stage of an Olympus BHSM microscope, which is equipped with 10x, 20x, and 50x objective lenses, for the 298 K measurements. No further sample preparation was needed in terms of cleaning or removing remaining parts of the host-rock. The microscope is part of a Renishaw 1000

Raman microscope system, which also includes a monochromator, a filter system and a CCD as the detector. Raman spectra were excited by a Spectra-Physics model 127 He-Ne laser (633 nm) at a resolution of 2 cm^{-1} in the range between 500 and 1500 cm^{-1}. Repeated acquisition using the highest magnification were accumulated to improve the signal to noise ratio in the spectra. Spectra were calibrated using the 520.5 cm^{-1} line of a silicon wafer. The cleanest crystal was selected for the more detailed study reported in this paper.

Spectra at liquid nitrogen temperature (77 K) and for comparison at 293 K were obtained using a Linkam thermal stage (Scientific Instruments Ltd, Waterfield, Surrey, England). The single crystal was placed on a circular glass disc (in a fixed orientation), which fitted over the silver plate of the thermal stage. Because of the increased optical path, spectra are noisier and require longer accumulation times compared to the normal Raman microscope set-up as described in the previous paragraph. Spectra were obtained using 20 seconds scans for up to 30 minutes

Table 2. Chemical analyses (JEOL 840A Electron Probe Microanalyser) of the celestine from Winterswijk.

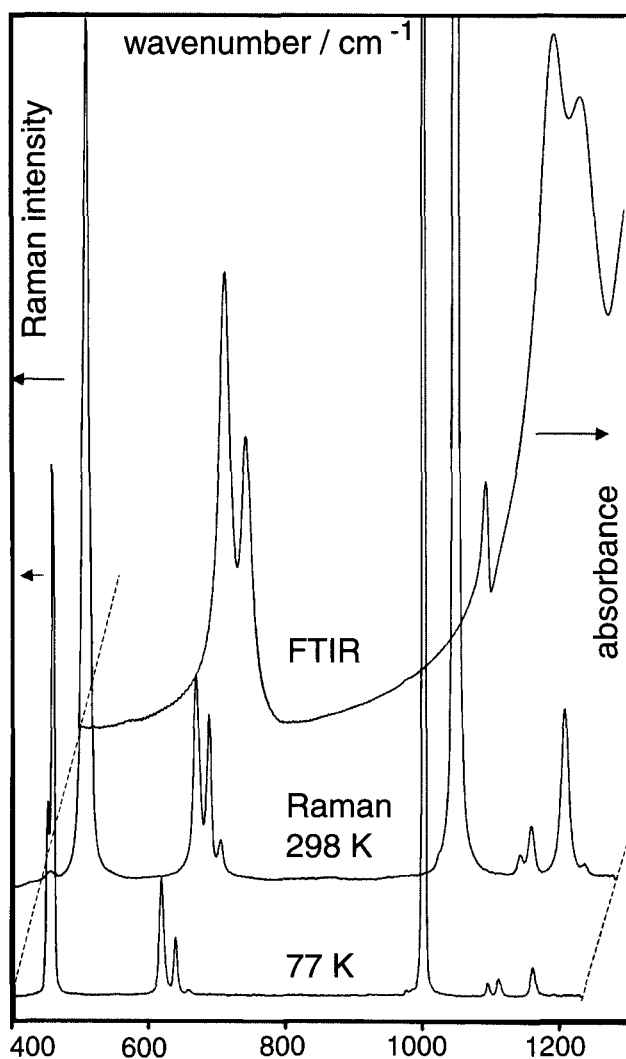|	Large celestine crystals				Secondary Sr-Ba phase		
Element	Theoretical weight%	Weight%	Atom%		Element	Weight%	Atom%
S	17.4	13.63	14.33		S	8.260	11.68
Ca	–	0.030	0.02		Ca	0.060	0.06
Fe	–	0.040	0.02		Fe	0.060	0.05
Sr	47.8	54.43	20.95		Sr	18.27	9.46
Ba	–	1.39	0.34		Ba	61.64	17.06
O	34.8	30.51	29.48		O	21.74	4.21

Fig. 2. FT-IR and Raman spectra at 293 K and 77 K of celestine in the region between 400 and 1300 cm⁻¹.

using the special short 50X (UWLD) objective. A lower Raman signal was obtained using this objective owing to the low numerical aperture of this long working distance objective. This, combined with the spherical aberration of the stage window, results in a decreased signal compared with that run without the thermal stage.

Spectral manipulations

Spectral manipulation such as baseline adjustment, smoothing and normalisation of both the IES and Raman spectra were performed using the Spectracalc software package GRAMS (Galactic Industries Corporation, NH, USA). Band component analysis was undertaken using the Jandel 'Peakfit' software package, which enabled the type of fitting function to be selected and allows specific parameters to be fixed or varied accordingly. Band fitting was done using a Lorentz-Gauss cross-product function with the minimum number of component bands used for the fitting process. The Gauss-Lorentz ratio was maintained at values greater than 0.7 and fitting was undertaken until reproducible results were obtained with squared correlations of r^2 greater than 0.995.

Results and discussion

The normal IR absorption spectrum and the Raman spectra at 293 and 77 K are shown in Figure 1. The results are summarized and compared to literature values in Table 3. The strong frequencies at 1201, 1138 and 1091 cm⁻¹ are due to the triply asymmetric

Table 3. Band component analysis of the IR and Raman spectra of celestine.

IR this study/cm⁻¹	IR (Gadsden 1975)/cm⁻¹	IR (Omori 1968)/cm⁻¹	IR (Guirguis 1987)/cm⁻¹	IR (Ross1972, 1974)/cm⁻¹	Raman 293 K this study/cm⁻¹	Raman 77 K this study/cm⁻¹	Raman (Griffith 1987)/cm⁻¹	Assignment
1248	1240-1250							? (IR)
1201	1190-1207	1195	1200	1179	1187	1176	1185	ν_3 (IR + R) SO_4
1138	1131-1145	1130	1150	1147	1158	1162	1159	ν_3 (IR + R) SO_4
					1110	1112	1103	ν_3 SO_4 (R) SO_4
1091	1080-1096	1095	1110	1081	1093	1096	1094	ν_3 (IR + R) SO_4
						1003		ν_1 (R) SO_4
991	993-998	990	1015	974	1000	1001	999	ν_1 (IR + R) SO_4
643	641-644	639	650	642	656	659	656	ν_4 (IR + R) SO_4
				627	638	640	637	ν_4 (IR + R) SO_4
611	610-613	610	620	613	620	620	624	ν_4 (IR + R) SO_4
							617	ν_4 (R) SO_4
				491				ν_2 (IR) SO_4
					460	460	458	ν_2 (R) SO_4
					453	453	453	ν_2 (R) SO_4
							240	Sr-O
							190	Sr-O
							50	Sr-O

S-O stretching mode v_3. Although these three frequencies have been observed by several others (Omori 1968, Ross 1972, Ross 1974, Gadsden 1975, Guiguis 1987) quite a large variation in the exact band positions exists. These differences may be explained by the incorporation in the crystal structure of small amounts of Ba or minor amounts of Ca, as a complete solid-solution series exists between barite and celestine, while the solid solution with the Ca equivalent is very limited. Guirguis (1987) has shown that there is a strong correlation between the ionisation potential of Ba, Ca and Sr and the observed shift in frequency of the SO_4^{2-} stretching modes. However, the electron probe microanalyses have shown that this is not the case for the large celestine crystals from Winterswijk used in this study. Unclear at this stage is the origin of the minor shoulder at 1248 cm^{-1}. Similar variations can be observed for the other vibrational modes of the sulfate group. The non-degenerate O-S-O bending modes labelled v_4 occur at 643 and 611 cm^{-1}. According to the selection rules the v_1 mode should only be Raman active in the case of undistorted SO_4^{2-} tetrahedra, however a minor band can be observed in the infrared spectrum around 991 cm^{-1} confirming the decrease in symmetry. This is a general feature for many crystalline sulfate compounds. In addition, Ross (1972) also reports a band at 491 cm^{-1} as the v_2 mode. However, this band has not been reported by others and is not observed in our infrared spectrum either. The complete band component analysis of the region between 500 and 1400 cm^{-1} is shown in Figure 3.

The Raman spectrum at room temperature (293 K) shows much sharper bands than the infrared spectrum. Instead of the three bands in the infrared spectrum, the v_3 mode is represented by four bands at 1187, 1158, 1110 and 1093 cm^{-1} in the Raman spectrum. Cooling to liquid nitrogen temperature (77 K) results in minor shifts of approximately 2-5 cm^{-1} towards higher wavenumbers for three of the bands except for the 1187 cm^{-1} band, which shifts 11 cm^{-1} towards lower wavenumbers (Figure 4). Although the intensity of the bands diminished, a clear decrease in line-width from approximately 9.0-12.0 cm^{-1} to 5.5-7.5 cm^{-1} can be observed due to the lower thermal motion of the atoms in the crystal structure. Similarly, the v_4 mode represented by two bands in the infrared spectrum is degenerated to three bands at 656, 638 and 620 cm^{-1} in the Raman spectrum at room temperature. A much smaller shift of less than 3 cm^{-1} towards higher wavenumbers is observed for this mode upon cooling to 77 K accompanied by a decrease in linewidth from about 7.5-9.0 cm^{-1} to 5.5-7.0 cm^{-1} (Figure 5).

The v_1 SO_4^{2-} mode is, according to the selection rules, infrared inactive and Raman active when it is present as an undistorted tetrahedron. This mode
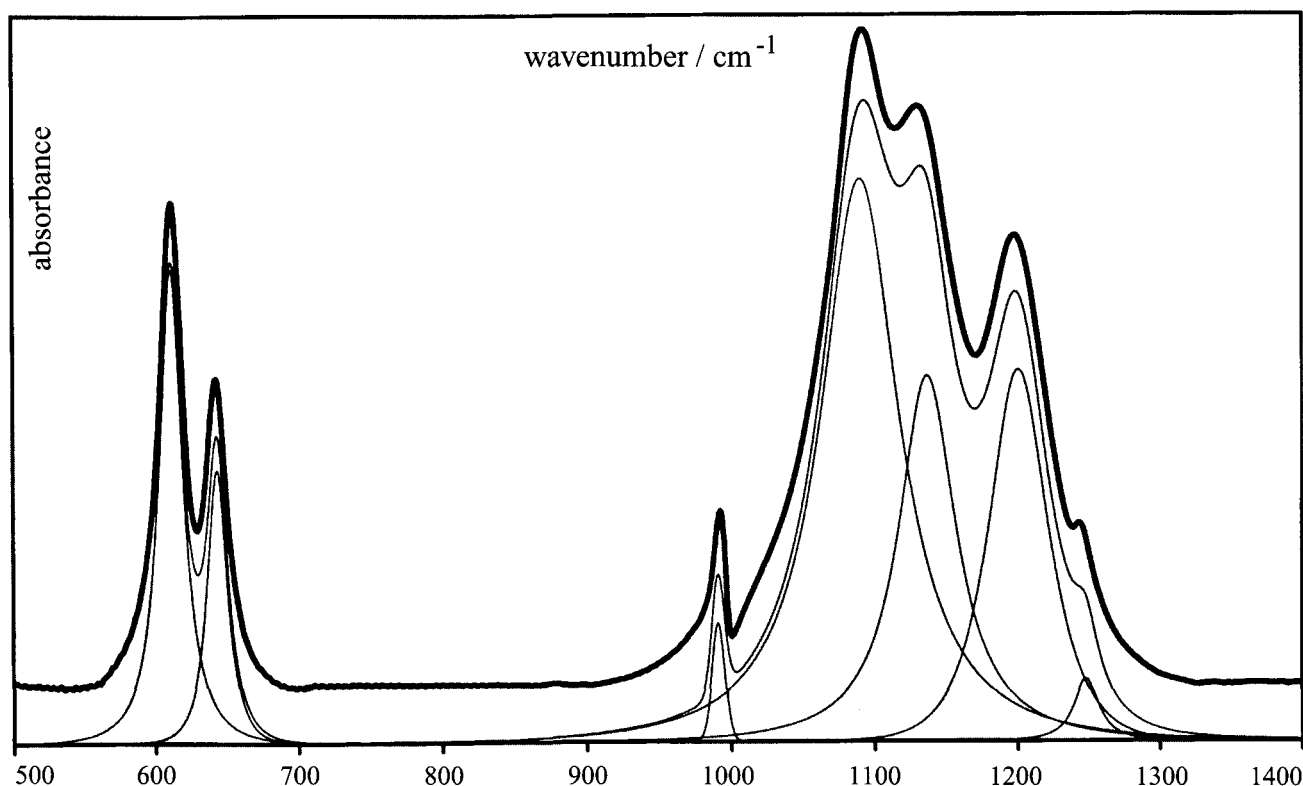

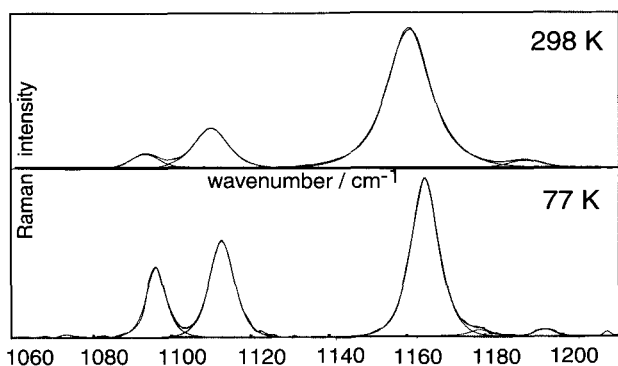Fig. 3. Band component analysis of the FT-IR region between 500 and 1400 cm^{-1}.

Fig. 4. Band component analysis of the Raman region between 1060 and 1210 cm⁻¹ at 293 K and 77 K.

Fig. 5. Band component analysis of the Raman region between 600 and 670 cm⁻¹ at 293 K and 77 K.

represents the strongest band in the Raman spectrum and is observed as a symmetric band at 1000 cm⁻¹. Upon cooling to 77 K this band becomes sharper but also asymmetric. Band component analysis suggests that this band represents not a single band but rather a highly overlapping double band at 1003 and 1001 cm⁻¹ (Figure 6).
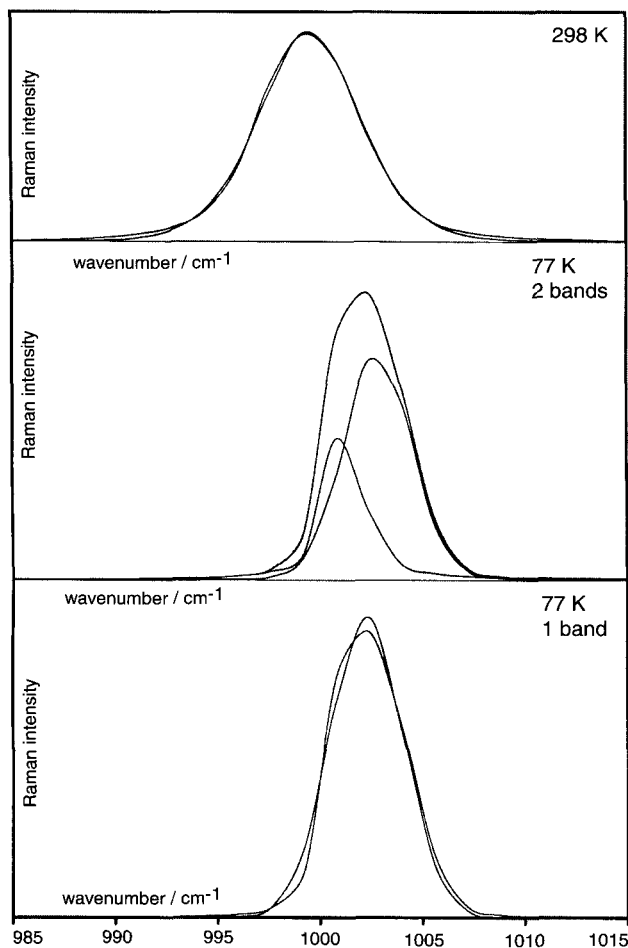
The bandwidth decreased from 5.7 cm⁻¹ for the 1000

Fig. 6. Band component analysis of the Raman region between 985 and 1015 cm⁻¹ at 293 K and 77 K with the 77 K spectrum fitted with one and with two bands.

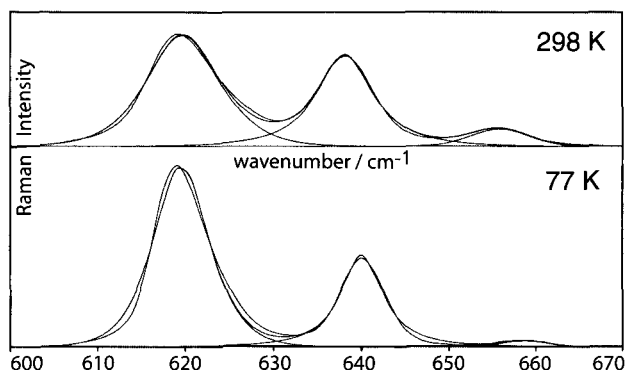cm⁻¹ band at room temperature to 3.8 and 1.6 cm⁻¹ for the 1003 and 1001 cm⁻¹ bands at 77 K, respectively. This split has not been observed before in the room temperature Raman spectra due to the strong overlap of these two bands. The shift of both overlapping bands in opposite directions together with a narrowing of both bands caused by the cooling to 77 K makes it possible to observe both bands. The v_2 mode is observed as a band around 460 cm⁻¹ with a difficult to see shoulder at 453 cm⁻¹. No shift is observed due to cooling from 293 K to 77 K, although the bands become sharper and the two bands become visible as separate bands (Figure 7). The bandwidth decreases from approximately 8.0 cm⁻¹ to 4-5 cm⁻¹ upon cooling to 77 K.

Cooling from room temperature (293 K) to liquid nitrogen temperature (77 K) results in a general decrease in intensity of all observed bands. This can be explained by changes in the crystal structure of the celestine. Generally cooling of a solid material results in a reduction of the various bondlengths between atoms. In the case of celestine this will result in a movement of the large cation Sr towards one or more of the oxygen atoms in the sulfate group. This movement will have a distinctive effect on the polarisability
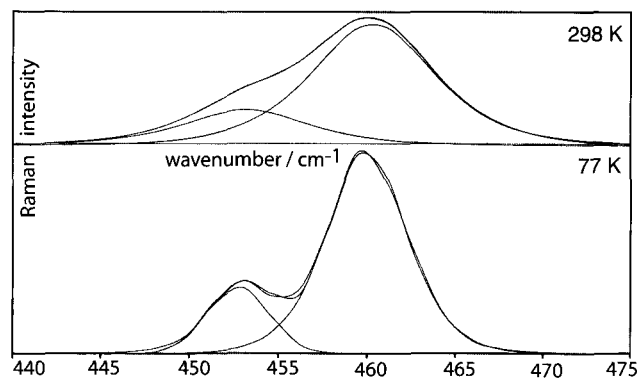

Fig. 7. Band component analysis of the Raman region between 440 and 475 cm⁻¹ at 293 K and 77 K.

and coupled to this effect it will cause a decrease in intensity. The facts that not all bands decrease equally in intensity indicates that not all oxygen atoms of the sulfate are influenced in the same way by the movement of the Sr cation.

Acknowledgements

References

Adler, H.H. & Kerr, P.F. 1965. Variations in IR spectra, molecular symmetry and site symmetry of sulphate minerals. Am. Miner. 50: 132-147

Gadsden, J.A. 1975. Infrared Spectra of Minerals and Related Inorganic Compounds. Butterworth & Co. (Publishers) Ltd., London, 277 pp

Griffith, W.P. 1987. Advances in the Raman and Infrared spectroscopy of minerals. In: Spectroscopy of Inorganic-based materials, R.J.H. Clark and R.E. Hester (eds.), John Wiley & Sons Ltd., 119-186

Guirguis, L.A. 1987. Infrared vibrational sulphate band shift correlation in alkaline sulphate minerals. TIZ-Fachberichte 111: 339-340

Habers, E.G.F. 1982. Coelestin aus Holland. Parallelfasiger Coelestin als Spaltenfüllung im Muschelkalk. Lapis 10: 24

Habers, E.G.F. & Tangerding, M. 1975. Coelestienkristallen uit de Muschelkalk van Winterswijk. Grondboor en Hamer 4: 130-136

Kloprogge, J.T. & Frost, R.L. 1999a. Raman microscopy at 77 K of natural gypsum $CaSO_4.2H_2O$. J. Mater. Science Letters, 19(3), 229-231

Kloprogge, J.T. & Frost, R.L. 1999b. Raman microscopy study of basic aluminum sulfate – J. Mater. Science 34: 4199-4202

Kloprogge, J.T. & Frost, R.L. 1999c. Raman microscopy study of basic aluminum sulfate. Part II. Raman microscopy at 77 K. J. Mater. Science, 34, 4367-4374.

Omori, K. 1986. Infrared diffraction and the far infrared spectra of anhydrous sulfates. Miner. J. 5: 334-354

Oosterink, H.W. 1986. Winterswijk, Geologie deel II. De Trias-periode (geologie, mineralen en fossielen). Wetenschappelijke mededelingen K.N.N.V. 178, 120 pp

Peletier, W. & Kolstee, H.G. 1986. Winterswijk, Geologie deel I. Inleiding tot de geologie van Winterswijk. Wetenschappelijke mededelingen K.N.N.V. 175: 136 pp

Ross, S.D. 1972. Inorganic Infrared and Raman Spectra. McGraw-Hill Book Company (UK) Ltd., London, 414 pp

Ross, S.D. 1974. Sulphates and other oxy-anions of group VI. In: The Infrared Spectra of Minerals, V.C. Farmer (ed.), Miner. Soc. Monogr. 4: 423-444

Rull, F., Lopez, F., Arana, R., Alia, J., Prieto, A.C. & Acosta, A. 1989. Caracterizacion de algunas celestinas Espanolas por espectroscopia Raman e IR. Bol. Soc. Esp. Miner. 12: 169-178.